Dynamic crack propagation in decagonal Al–Ni–Co quasicrystal

2008 J. Phys.: Condens. Matter 20 295217

(http://iopscience.iop.org/0953-8984/20/29/295217)

IOP Publishing Journal of Physics: Condensed Matter

J. Phys.: Condens. Matter **20** (2008) 295217 (9pp) doi:10.1088/0953-8984/20/29/295217

Dynamic crack propagation in decagonal Al–Ni–Co quasicrystal

Ai-Yu Zhu[1] **and Tian You Fan**[2]

[1] Department of Mathematics, School of Science, Beijing Institute of Technology, Beijing 100081, People's Republic of China

[2] Department of Physics, School of Science, Beijing Institute of Technology, PO Box 327, Beijing 100081, People's Republic of China

E-mail: aiyuzhu@yahoo.com.cn

Received 23 January 2008, in final form 27 May 2008
Published 1 July 2008
Online at stacks.iop.org/JPhysCM/20/295217

Abstract

The appearance of unusual internal variables—phason degrees—in quasicrystals challenges the traditional theory of condensed matter in macro- as well as in microscopy, especially for a dynamic process. The elasto-/hydrodynamic model for quasicrystals is suggested and investigated. With this model and the finite difference method the wave propagation and diffusion and their interaction through a cracked sample are revealed in this study. Even though the phason degrees of freedom present the diffusion nature according to the present model, this influences the dynamic process greatly. The influences are different for dynamic initiation of crack growth and fast crack propagation; for the latter the nonlinear effect—moving boundary effect—is evident as well as the wave propagation effect, diffusion effect and phonon–phason coupling effect.

(Some figures in this article are in colour only in the electronic version)

1. Introduction

Quasicrystals as a new material possess unusual degrees of freedom named 'phason degrees of freedom', which influence many physical properties, in particular mechanical ones. The degrees of freedom are described by a vector field with values in an internal 'orthogonal space'. A gradient of this field forms the phason strain tensor describing atom local rearrangement, which together with the conventional 'phonon' strain tensor describing volume and shape change of a unit cell can be incorporated into a generalized free energy of the elastic solid containing phonon elastic constants, phason elastic constants and phonon–phason coupling elastic constants.

Since the discovery of quasicrystals, almost all scholars agree on the form of the generalized static elasticity theory, but for the elasto-/hydrodynamic case there are different theoretical points of view, e.g. those being put forward by Bak [1, 2] and by Lubensky *et al* [3]. Both of their arguments are in agreement with the deformation geometry and generalized Hooke's law; the difference between them lies in the equations of motion. Ding *et al* [4], Fan *et al* [5–7], and Li and Liu [8] followed Bak's arguments, that is, both phonon and phason describe wave propagation, i.e.

$$\rho\frac{\partial^2 u_i}{\partial t^2} = \frac{\partial \sigma_{ij}}{\partial x_j} \qquad \rho\frac{\partial^2 w_i}{\partial t^2} = \frac{\partial H_{ij}}{\partial x_j} \tag{1}$$

in which u_i and w_i are the phonon displacement vector and phason displacement vector, σ_{ij} and H_{ij} are the phonon stress tensor and phason stress tensor, and ρ is the mass density of the material, respectively. Although they reviewed the work of Lubensky *et al*, maybe they found that in this version the discussion is easier and more beneficial to develop an analytical solution for various boundary or boundary–initial value problems. Rochal and Lorman [9] supported the argument and suggested that in the second equation of (1) the density ρ should be replaced by ρ_{eff}, where ρ_{eff} represents the generalized effective phason density, but the meaning of the quantity is not so clear and its measurement is difficult. Afterwards in [10] they considered the argument of Lubensky *et al* and suggested that people should compromise between different models, e.g. those proposed by [3] and [4]. At present not enough experimental data are available to examine each

model. However, if we use the common features of different models and find a simpler version for elasto-/hydrodynamics of quasicrystals, then carry out systematic theoretical, numerical and experimental work, this will be beneficial to promote the study. Based on this idea Fan *et al* [11] suggested a so-called elasto-/hydrodynamic model, and analytic solutions for moving dislocations in some quasicrystalline systems are achieved.

In the following sections, the elasto-/hydrodynamic equations with equations of deformation geometry and generalized Hooke's law under appropriate boundary–initial conditions are solved in terms of the finite difference method. Numerical results for the problem of dynamic initiation of crack growth and fast crack propagation are given.

2. Elasto-/hydrodynamic equations and boundary–initial conditions of two-dimensional decagonal quasicrystals

Phonon strain components ε_{ij} and phason strain components w_{ij} are defined by

$$\varepsilon_{ij} = (\partial_j u_i + \partial_i u_j)/2, \qquad w_{ij} = \partial_j w_i, \qquad \partial_j = \partial/\partial x_j \tag{2}$$

where u_i and w_i are phonon and phason displacement vectors, respectively, as mentioned above.

According to Ding *et al* [4], phonon stress components σ_{ij} and phason stress components H_{ij} have the following relation with the corresponding strain components ε_{ij} and w_{ij}, i.e. the generalized Hooke's law for quasicrystals:

$$\begin{aligned} \sigma_{ij} &= C_{ijkl}\varepsilon_{kl} + R_{ijkl}w_{kl} \\ H_{ij} &= K_{ijkl}w_{kl} + R_{klij}\varepsilon_{kl} \end{aligned} \tag{3}$$

where C_{ijkl} and K_{ijkl} are the elastic constants of the phonon and phason fields and R_{klij} are the phonon–phason coupling elastic constants, respectively. These elastic constants have been derived by group representation theory.

Collaborating arguments of Bak and Lubensky *et al*, under linear and small deformation, the equations of motion are

$$\begin{aligned} \rho\frac{\partial^2 u_i}{\partial t^2} &= \frac{\partial \sigma_{ij}}{\partial x_j} \\ \kappa\frac{\partial w_i}{\partial t} &= \frac{\partial H_{ij}}{\partial x_j} \end{aligned} \tag{4}$$

in which ρ is the mass density, $\kappa = 1/\Gamma_w$ and the kinematic coefficient Γ_w of the phason field of the material is defined by Lubensky *et al* [3].

It is obvious that the first equation of equation set (4) is the equation of conventional elastodynamics, which is the same as the first equation of equation set (1), while the second one is the diffusion equation. The second equation of (4) is a linear result of hydrodynamics of quasicrystals proposed by Lubensky *et al*. The dynamic equation (4) should be named the elasto-/hydrodynamic equations for quasicrystals, which are identical to equations (5) of [10]. We believe this treatment is more fundamental physically and harmonizes the contradiction between the arguments of Bak and Lubensky *et al*. It also harmonizes the contradiction between [4–8] and [9], though they in common follow the framework of Bak's argument.

Among 200 kinds of quasicrystals observed to date, there are 100 kinds of three-dimensional icosahedral quasicrystals and 70 kinds of two-dimensional decagonal quasicrystals; these two kinds of solid phases constitute the majority of the material and play a central role. For simplicity, here only a two-dimensional decagonal quasicrystal will be considered. We denote the periodic direction as the z axis and the quasiperiodic plane as the x–y plane. Assume that a Griffith crack penetrates through the solid along the periodic direction, i.e. the z axis. It is obvious that elastic field induced by a uniform tensile stress at upper and lower surfaces of the specimen is independent of z, so all field variables are independent of z, i.e., $\partial/\partial z = 0$. In this case, the stress–strain relations are reduced to

$$\begin{aligned} \sigma_{xx} &= L(\varepsilon_{xx} + \varepsilon_{yy}) + 2M\varepsilon_{xx} + R(w_{xx} + w_{yy}) \\ \sigma_{yy} &= L(\varepsilon_{xx} + \varepsilon_{yy}) + 2M\varepsilon_{yy} - R(w_{xx} + w_{yy}) \\ \sigma_{xy} &= \sigma_{yx} = 2M\varepsilon_{xy} + R(w_{yx} - w_{xy}) \\ H_{xx} &= K_1 w_{xx} + K_2 w_{yy} + R(\varepsilon_{xx} - \varepsilon_{yy}) \\ H_{yy} &= K_1 w_{yy} + K_2 w_{xx} + R(\varepsilon_{xx} - \varepsilon_{yy}) \\ H_{xy} &= K_1 w_{xy} - K_2 w_{yx} - 2R\varepsilon_{xy} \\ H_{yx} &= K_1 w_{yx} - K_2 w_{xy} + 2R\varepsilon_{xy} \end{aligned} \tag{5}$$

where $L = C_{12}$, $M = (C_{11} - C_{12})/2$ are the phonon elastic constants, K_1 and K_2 are the phason elastic constants, and R the phonon–phason coupling elastic constant.

Substituting (5) into (4), we obtain the equations of motion of decagonal quasicrystals as follows:

$$\begin{aligned} &\frac{\partial^2 u_x}{\partial t^2} + \theta\frac{\partial u_x}{\partial t} = c_1^2\frac{\partial^2 u_x}{\partial x^2} + (c_1^2 - c_2^2)\frac{\partial^2 u_y}{\partial x\,\partial y} + c_2^2\frac{\partial^2 u_x}{\partial y^2} \\ &\qquad + c_3^2\left(\frac{\partial^2 w_x}{\partial x^2} + 2\frac{\partial^2 w_y}{\partial x\,\partial y} - \frac{\partial^2 w_x}{\partial y^2}\right) \\ &\frac{\partial^2 u_y}{\partial t^2} + \theta\frac{\partial u_y}{\partial t} = c_2^2\frac{\partial^2 u_y}{\partial x^2} + (c_1^2 - c_2^2)\frac{\partial^2 u_x}{\partial x\,\partial y} + c_1^2\frac{\partial^2 u_y}{\partial y^2} \\ &\qquad + c_3^2\left(\frac{\partial^2 w_y}{\partial x^2} - 2\frac{\partial^2 w_x}{\partial x\,\partial y} - \frac{\partial^2 w_y}{\partial y^2}\right) \\ &\frac{\partial w_x}{\partial t} + \theta w_x = d_1^2\left(\frac{\partial^2 w_x}{\partial x^2} + \frac{\partial^2 w_x}{\partial y^2}\right) \\ &\qquad + d_2^2\left(\frac{\partial^2 u_x}{\partial x^2} - 2\frac{\partial^2 u_y}{\partial x\,\partial y} - \frac{\partial^2 u_x}{\partial y^2}\right) \\ &\frac{\partial w_y}{\partial t} + \theta w_y = d_1^2\left(\frac{\partial^2 w_y}{\partial x^2} + \frac{\partial^2 w_y}{\partial y^2}\right) \\ &\qquad + d_2^2\left(\frac{\partial^2 u_y}{\partial x^2} + 2\frac{\partial^2 u_x}{\partial x\,\partial y} - \frac{\partial^2 u_y}{\partial y^2}\right) \end{aligned} \tag{6}$$

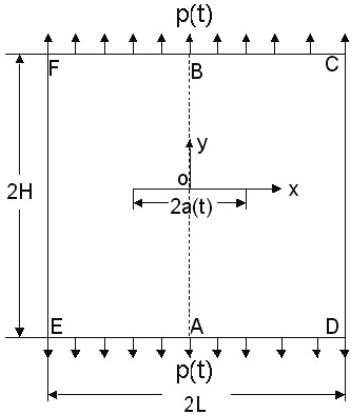

Figure 1. The specimen with a rest or propagating crack.

in which

$$c_1 = \sqrt{\frac{L+2M}{\rho}}, \qquad c_2 = \sqrt{\frac{M}{\rho}}, \qquad c_3 = \sqrt{\frac{R}{\rho}},$$
$$d_1 = \sqrt{\frac{K_1}{\kappa}}, \qquad d_2 = \sqrt{\frac{R}{\kappa}}, \qquad d_3 = \sqrt{\frac{K_2}{\kappa}}; \tag{7}$$

note that constants c_1, c_2 and c_3 have the meaning of elastic wave speeds, while d_1^2, d_2^2 and d_3^2 do not represent wave speed; they are diffusive coefficients.

In equation (6), parameter θ may be understood as a man-made damping coefficient; if it is equal to zero, they obviously return to the dynamic state, whereas if $\theta > 0$, which successively is adjusted to an appropriate value, so that the terms of the left-hand side of equation (6) are zero, then we obtain the corresponding static solution, which can easily be examined with well known solutions. If the examination confirms that the scheme and computer program are correct and of sufficient precision then we put $\theta = 0$, and begin the dynamic computation.

Consider a decagonal quasicrystal with a Griffith crack shown in figure 1. It is a rectangular specimen with a central crack of length $2a(t)$ subjected to a dynamic tensile stress at its ends ED and FC, in which $a(t)$ represents the crack length, being a function of time in general. For dynamic initiation of crack growth the crack is stable, so $a(t) = a_0 =$ constant, while for fast crack propagation $a(t)$ varies with time. At first we consider dynamic initiation of crack growth, then study fast crack propagation. Due to the symmetry of the specimen only the upper right quarter is considered.

Referring to the upper right part and considering a fix grips case, the following boundary conditions should be satisfied (in the general case the tractions for phonon variables and the generalized tractions for phason variables must be simultaneously included in the boundary conditions; due to a lack of measured data for the generalized tractions, the phason stress boundary conditions are taken to be zero for simplicity):

$$\begin{aligned}
&u_x = 0, \qquad \sigma_{yx} = 0, \qquad w_x = 0, \qquad H_{yx} = 0 \\
&\quad \text{on } x = 0 \text{ for } 0 \leqslant y \leqslant H \\
&\sigma_{xx} = 0, \qquad \sigma_{yx} = 0, \qquad H_{xx} = 0, \qquad H_{yx} = 0 \\
&\quad \text{on } x = L \text{ for } 0 \leqslant y \leqslant H \\
&\sigma_{yy} = p(t), \qquad \sigma_{xy} = 0, \qquad H_{yy} = 0, \qquad H_{xy} = 0 \\
&\quad \text{on } y = H \text{ for } 0 \leqslant x \leqslant L \\
&\sigma_{yy} = 0, \qquad \sigma_{xy} = 0, \qquad H_{yy} = 0, \qquad H_{xy} = 0 \\
&\quad \text{on } y = 0 \text{ for } 0 \leqslant x \leqslant a(t) \\
&u_y = 0, \qquad \sigma_{xy} = 0, \qquad w_y = 0, \qquad H_{xy} = 0 \\
&\quad \text{on } y = 0 \text{ for } a(t) < x \leqslant L
\end{aligned} \tag{8}$$

in which $p(t)$ is the dynamic load. In this paper $p(t) = p_0 f(t)$, where $f(t)$ is the Heaviside function and $p_0 =$ const with the stress dimension.

The initial conditions are

$$\begin{aligned}
&u_x(x, y, t)|_{t=0} = 0 \qquad u_y(x, y, t)|_{t=0} = 0 \\
&w_x(x, y, t)|_{t=0} = 0 \qquad w_y(x, y, t)|_{t=0} = 0 \\
&\left.\frac{\partial u_x(x, y, t)}{\partial t}\right|_{t=0} = 0 \qquad \left.\frac{\partial u_y(x, y, t)}{\partial t}\right|_{t=0} = 0.
\end{aligned} \tag{9}$$

Through the constitutive equation (5), boundary conditions (8) which involve stresses are expressed in terms of displacements and their derivatives, so the final version of differential equation (6) and both conditions (8) and (9) are expressed by the displacements.

For the related parameters in a decagonal Al–Ni–Co quasicrystal, the experimentally measured data $\rho = 4.186 \times 10^{-3}$ g mm^{-3} are used and elastic moduli are taken as $C_{11} = 2.3430$, $C_{12} = 0.5741(10^{12}$ dyn cm$^{-2})$, which are obtained by resonant ultrasound spectroscopy [12]; we have also chosen $K_1 = 1.22$ and $K_2 = 0.24(10^{12}$ dyn cm$^{-2})$ estimated by Monte Carlo simulation [13] and $\Gamma_w = 1/\kappa = 4.8 \times 10^{-10}$ cm^3 μs g^{-1} [14]. The coupling constant R has not been measured so far. In computation we take $R/M = 0.01$ as the coupling case corresponding to quasicrystals, and $R/M = 0$ as the decoupled case, corresponding to crystals if simultaneously $K_1 = 0$, $K_2 = 0$. In the following sections 3–6, $H = 20$ mm, $L = 10$ mm and the crack initial length $a_0 = 2.4$ mm.

3. Stability and accuracy of the finite difference scheme

Equation (6) subjected to conditions (8) and (9) is very complicated and an analytic solution for the boundary–initial value problem is not available at present, which has to be solved by the numerical method. Here we extend the finite difference method of the Shmuely–Alterman [15] scheme for analyzing the crack problem for conventional engineering materials to quasicrystalline materials. There are also some other numerical approaches to work out the problems; see [16].

A grid is imposed on the upper right of the specimen shown in figure 2. For convenience, the mesh size (also called the space step) h is taken to be the same in both x and y directions. The grid is extended beyond the half step by adding four special grid lines $x = -h/2, x = L + h/2, y = -h/2, y = H + h/2$, which form the grid

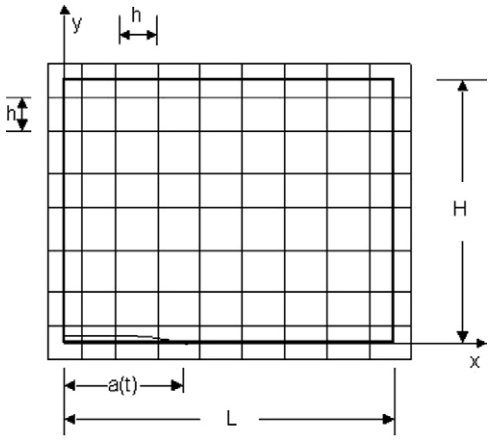

Figure 2. Scheme of the grid used.

boundaries. Denoting the time step by τ, central difference approximations are used to discretize equations (6) and (9). In constructing the difference of boundary conditions (8) we follow a method proposed by Alterman and Rotenberg [17], which was also successfully employed in [18, 19] of periodic crystals. According to this method, derivatives perpendicular to the boundary are proposed by non-central differences and derivatives parallel to the boundary by a centered difference. The real boundary can be considered to be located at a distance of half the mesh size from the grid boundaries (see figure 2). The detail of the finite difference scheme is omitted here to save space.

In relation to the fourth equation of equation set (6), the crack tip is confined to lie on the interval $c - h/2 < x < c + h/2$, in which c denotes the distance from the y-axis to the midpoint of the grid interval. As will become obvious later, any assumption concerning the exact location of the crack tip has no meaningful results or conclusions drawn from the numerical solution. The only occasion where it may have any significance is when comparing numerical and experimental results. In this case, however, it is the complete crack length which counts, so that any error introduced in locating the crack tip may be approximately assumed as being located in the middle of the above mentioned interval. By adhering to the assumption (which means that the value of c may be identified with the crack length a_0), the error introduced in estimating the crack length cannot exceed $h/2$. If, in addition, we refine the grid, the relative error can be reduced to at least the same degree as the expected experimental errors.

The stability of the algorithm is the core problem for the computation, which depends upon the choice of parameter $\alpha = c_1\tau/h$, which is the ratio between time step and space step substantively. The choice is related to the ratio c_1/c_2, i.e. the ratio between speeds of elastic longitudinal and transverse waves of the phonon field. To determine the upper bound for the ratio to guarantee the stability, according to our computational practice and considering the experiences of computation for conventional materials [20], we choose $\alpha = 0.8$ in all cases.

The correctness of the algorithms can be easily proved via the static solution first. As mentioned above, the numerical solution tends to the static solution if θ (see equation (6)) is taken as an appropriate value and the left-hand side of the equations to be zero. After some trials, the value is $0.05/h$.

In the following we first examine the physical model of the study, otherwise all computations will lose their meaning.

4. Examination on the model and algorithm

In this section we further verify our model from the point of view of mathematical physics. To verify the physical nature of the model, we first compute an un-cracked specimen. We know that there are fundamental solutions of pure wave equations and pure diffusion equations in classical mathematical physics; these solutions are ones in an infinite body, without initial conditions and without boundary conditions, characterizing time variation natures of wave propagation and diffusion, respectively, so that these fundamental solutions cannot describe wave reflection, diffraction caused by the finite boundary and the coupling effect between phonons and phasons and so on; they are as follows:

$$\begin{aligned} \text{solution}_{\text{wave}} &\sim \mathrm{e}^{\mathrm{i}\omega(t-x/c)} \\ \text{solution}_{\text{diffusion}} &\sim \frac{1}{\sqrt{t-t_0}}\mathrm{e}^{-(x-x_0)^2/\Gamma_w(t-t_0)} \end{aligned} \tag{10}$$

where the frequency and speed of the wave are denoted by ω and c, respectively. The solutions (10) provide a comparison for checking the basic nature of wave propagation for phonons and the basic nature of diffusion of phasons in the dynamic process predicted by the basic equation (4).

The comparison between our numerical results and the fundamental solution is given in figures 3(a)–(c), in which the dotted line represents the numerical solutions of real quasicrystals (i.e., the phonon and phason are coupled), the solid line stands for the solutions of the 'decoupled quasicrystals' and the dashed line corresponds to fundamental solutions (10) of mathematical physics. We can see, from figures 3(a) and (b), that both displacement components of the phonon field are identical to the fundament solutions and they demonstrate the wave propagation nature of phonon variables. Nevertheless, some differentiation is shown in the three curves of each picture, because the actual solutions (i.e. the numerical solutions) are subjected to the initial and boundary conditions, and influenced by the phonon–phason coupling effect, so they can not completely be in agreement with the fundamental solutions of mathematical physics. At first, there is some dissimilarity between numerical solutions (including numerical solutions of quasicrystals and numerical solutions of 'decoupled quasicrystals') and the fundamental solutions in the shape of the curves, as the former is influenced by initial and boundary conditions, while the latter is the solutions independent from any initial and boundary conditions. In addition, we also find that the solutions of real quasicrystals and solutions and 'decoupled quasicrystals' have some distinctions caused by the coupling effect, though they have similar shapes.

As for figure 3(c), in the phason field, the numerical solution of real quasicrystals presents a diffusive nature in

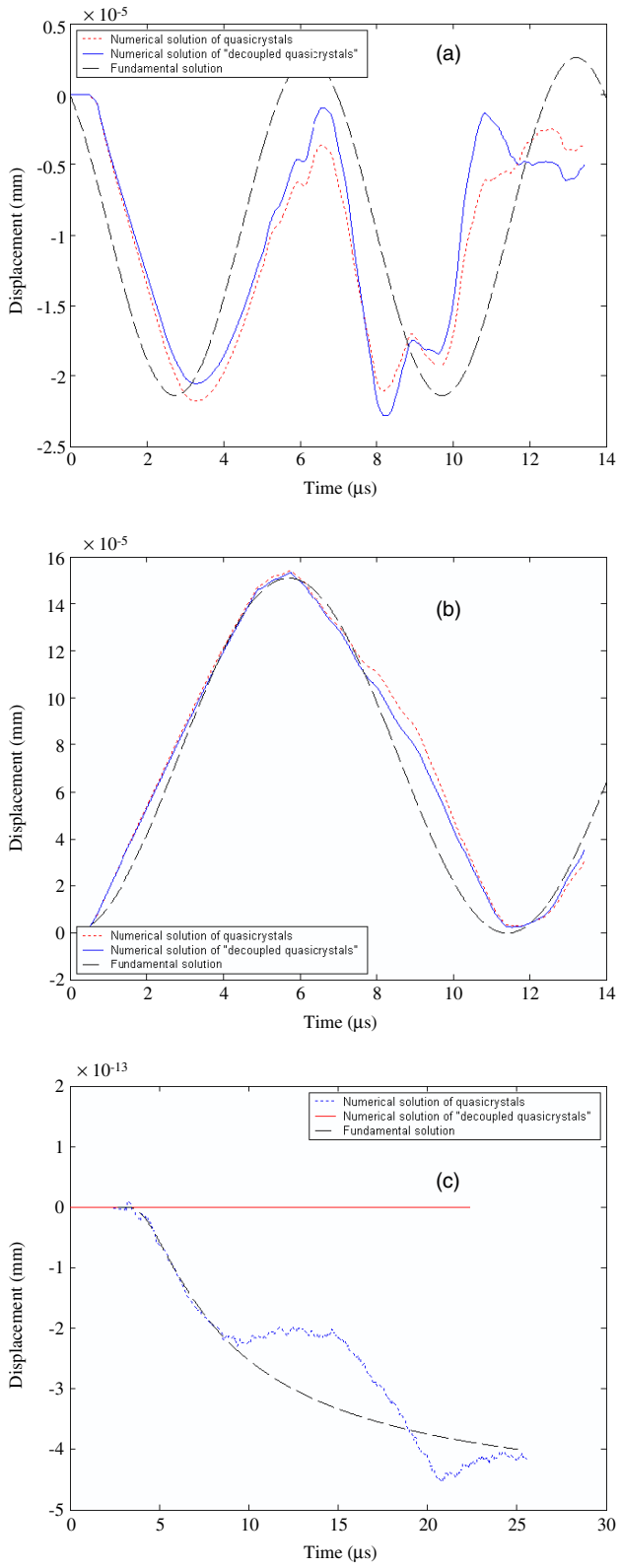

Figure 3. (a) Displacement component of phonon field u_x versus time. (b) Displacement component of phonon field u_y versus time. (c) Displacement component of phason field w_x versus time.

the overall tendency. Nevertheless, because of the influence of boundary conditions and the phonon and phonon–phason coupling effect, it also has some character of fluctuation. In the time interval between 5 and 10 μs, the numerical solution is a good match with the fundamental solution, and the numerical solution is a plateau in the time interval from 10 to 15 μs. However, after 15 μs, the curve repeats the tendency in 5 to 15 μs. Due to the limitation of the computer, we just draw up to 30 μs. Moreover, we observe that the numerical solution of the phason of the 'decoupled quasicrystals' is equal to zero, apparently different from the numerical solution of real quasicrystals and the fundamental solution. This is reasonable, since no other force (the generalized traction is assumed to be zero) is imposed upon the boundary condition and the only one comes from the coupling effect, without which the phason displacement should be zero.

At the first time step there is evidence of a phase shift between the quasicrystal solutions and the pure wave solution of mathematical physics shown by figure 3; the reason for this is that the specimen is a finite size sample: the wave propagation from the upper or lower external boundary of the specimen to the observed point needs time, which is less than 1 μs. We also notice that the numerical solution of displacements is constant up to about one minute. Because the force on the boundary is impact loading, the displacements increase or decrease sharply at about 1 μs when the wave from the external boundary arrives at the point we refer to.

The new scheme we proposed should be tested for its capability and accuracy. We can check the key physical quantity—dynamic stress intensity factor (DSIF), whose computational results can be compared with those of the well known solutions. Keeping in mind that the available experimental data in quasicrystals do not supply enough information, in order to compare with numerical results, we set the phonon–phason coupling constant R to be zero in equation set (6), with $R = 0$ the first two equations of equation set (6) are degenerated to the equations for crystals. The various parameters of the specimen were chosen to enable at least a qualitative and quantitative comparison with [21–23]; thus, the specimens were assumed to have $c_1 = 7.34, c_2 = 3.92$ (mm μs^{-1}) and $\rho = 5 \times 10^3$ kg m^{-3}, $p_0 = 1$ MPa.

The dynamic stress intensity factor $K_{\mathrm{I}}(t)$ is defined by

$$K_{\mathrm{I}}(t) = \lim_{x \to a_0^+} \sqrt{\pi (x - a_0)} \sigma_{yy}(x, 0, t) \tag{11}$$

and the normalized DSIF $\tilde{K}_{\mathrm{I}}(t) = K_{\mathrm{I}}(t)/\sqrt{\pi a_0} p_0$ is used.

An overall comparison between the results obtained in this paper and the classical analytic solution of Maue [21] and two numerical solutions given by Murti [22] and Chen [23] is plotted in figure 4. Maue's solution is the only exact analytic solution for crystal for dynamic initiation of crack growth so far, which studied a semi-infinite crack in an infinite elastic body, and the crack surface is subjected to the Heaviside loading. The configuration of Maue's problem is quite different from that of our problem; so is the boundary conditions. The differences are at least in three directions. (1) It is an infinite body; our object is a finite size specimen. (2) Its crack is semi-infinite; our crack is of finite size. (3) Its loading is subjected to the crack surface, and the loading in our specimen is applied at the external surface of the specimen. So Maue's solution cannot describe the stress wave propagation from the external

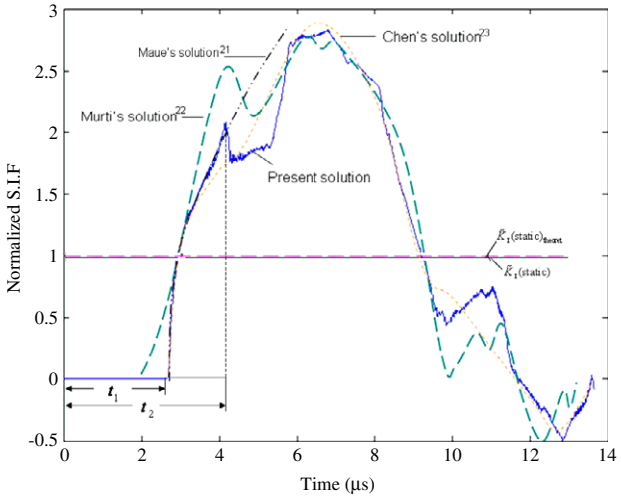

Figure 4. Normalized SIF versus time for crystals.

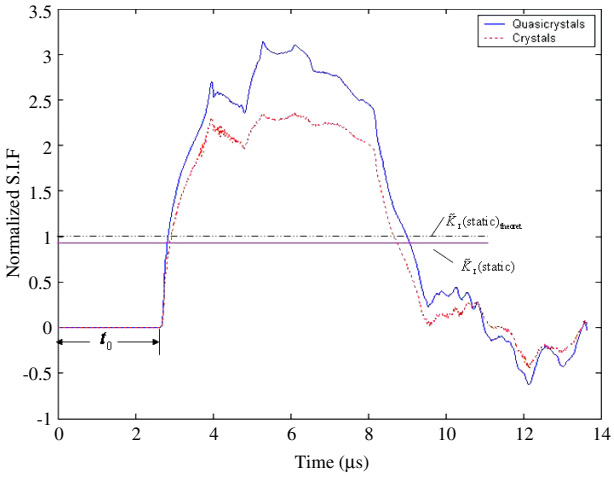

Figure 5. Normalized SIF versus time.

boundary of the finite size specimen, and cannot describe any interaction between the wave and external boundary, i.e. it can be used for our finite size specimen only in a very short time interval, during the period between the stress wave from the external boundary arriving at the crack tip (the time is denoted by $t_1 = 2.7248$ μs see figure 4) and before the reflection by the external boundary stress wave emanating from the crack tip in a finite size specimen (this time is marked by t_2, refer to figure 4, whose value is equal to $t_2 \approx 4.1$ μs). During this special very short time interval our specimen can be seen as an 'infinite specimen'. The comparison shows that our solution is in good agreement with Maue's solution within its validity period. From the overall tendency, the solution in this paper is in agreement with the numerical Murti's solution and Chen's solution too. However, there naturally are also some differences.

The comparison of our numerical solutions in the case without phason field with those of the well known classical analytic solution (Maue's solution) and numerical solutions (Murti's solution and Chen's solution) demonstrates that the finite difference method in the present study is a capable and reliable method. It is understandable that there are some small differences between the different numerical solutions, because they are all approximate solutions. This predicts that our method is a powerful one for solving problems of elasto-/hydrodynamics and fracture dynamics of quasicrystalline materials.

5. Results of dynamic initiation of crack growth

In dynamic fracture theory, there are two kinds of problems: dynamic initiation of crack growth and fast crack propagation. Sometimes one says these are two 'phases' of the problem. With regard to dynamic initiation of crack growth, the length of the crack is constant, assuming $a(t) = a_0$. The specimens with a stationary crack are subjected to a rapidly varying applied load $p(t) = p_0 f(t)$, where $f(t)$ is taken as the Heaviside function. It is well known the coupling effect between phonon and phason is very important, which reveals the distinctive physical properties including mechanical properties, and distinguishes quasicrystals from periodic crystals. So studying the coupling effect is significant.

In equation (6), by letting θ be equal to zero we obviously return to the dynamic state, whereas if $\theta > 0$ there are successive changes in displacements, converging finally to the static solution. The accuracy of the numerical scheme is checked via the static result.

There are four lines in figure 5: two straight lines, consisting of the numerical solution and the theoretical solution, representing the static ones of the quasicrystals, and the other are two curved lines, including quasicrystals and crystals, symbolizing the dynamic state. Concerning the static numerical stress intensity factor, $\tilde{K}(\text{static}) = 0.9418$, the error is 0.058 in contrast to the theoretical solution [24]. As to the dynamic solution shown in figure 5, we can see from the figure that the normalized DSIF of quasicrystals is evidently larger than that of crystals, though they are similar to some extent. We believe that the phason and phonon–phason coupling effects give rise to the fact that the DSIF of quasicrystals is big and this results in the mechanical properties of the quasicrystals being obviously different from those of conventional crystals. This also reveals that the effects of phason and phonon–phason coupling in the dynamic process are much stronger than those in the static process.

In figure 5, t_0 represents the time in which the wave from the external boundary propagates to the crack surface, where $t_0 = 2.6735$ μs. So the velocity of the wave propagation is $v = H/t_0 = 7.4807$ km s^{-1}, which is just equal to the longitudinal wave speed $c_1 = \sqrt{(L+2M)/\rho}$. This indicates that for the complex system of wave propagation and diffusion coupling, the phonon wave propagation plays a dominating role. At the moment that the wave arrives at the surface of the crack, because the dynamic load is an impacting force which produces a tensile wave, the DSIF increases sharply to the maximum. Then the DSIF steps into a smoother stage for period of time, and it starts to decrease steeply at about 8 μs, until at about 11 μs the DSIF drops to and below zero, because the tensile wave becomes a compressive wave, which yields the surface of the crack closing.

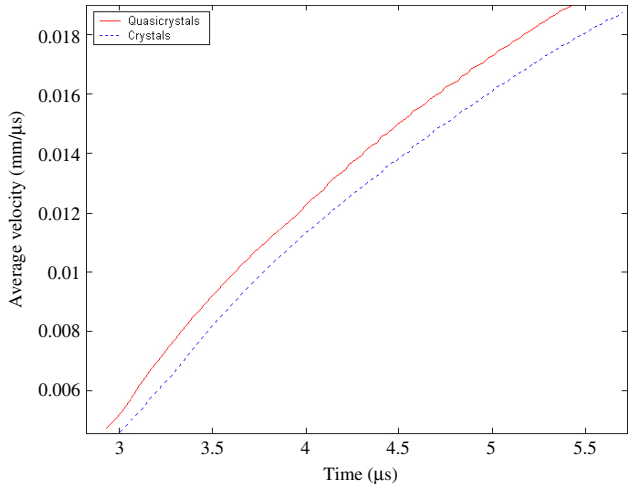

Figure 6. The average velocity of crack propagation versus time.

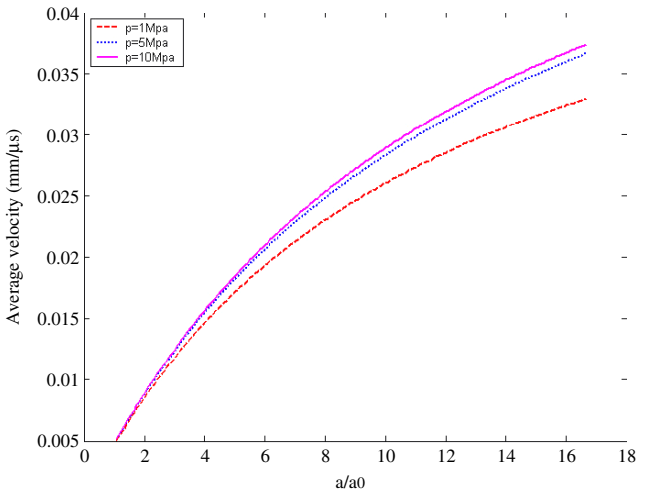

Figure 7. Variation of average velocity versus crack growth size for different load levels.

There are many oscillations in the figure, especially the dynamic stress intensity factor. These oscillations characterize the reflection and diffraction between waves coming from the crack surface and the sample's boundary surfaces. Meanwhile, these oscillations are greatly influenced by the material constants and specimen geometry, including the shape and sizes. Since the damping is ignored in the calculation, it has no effect on the oscillations.

Because current work in dynamic fracture mechanics is primarily based upon the assumption of linear elastic material behavior, the DSIF $K_{\mathrm{I}}(t)$ defined in equation (11) is meaningful only for linear elastic homogeneous (although not necessarily isotropic) materials which exhibit the $r^{-1/2}$ singularity at the tip of a sharp crack. With the calculated $K_{\mathrm{I}}(t)$ and an experimentally determined critical value of $K_{\mathrm{I}}(t)$ that is a material constant, we can set up a criterion for the dynamic initiation of crack growth, i.e.,

$$K_{\mathrm{I}}(t) = K_{\mathrm{Id}}(\dot{\sigma}, T) \tag{12}$$

where $K_{\mathrm{Id}}(\dot{\sigma}, T)$ is the so-called critical value of $K_{\mathrm{I}}(t)$ and is named the dynamic fracture toughness, which is dependent upon the loading rate $\dot{\sigma}$ and test temperature T. The DSIF is a computed quantity which does not represent the property of brittleness of the material. Of course, the brittleness of quasicrystals is indeed greater than that of crystals.

6. Preliminary results of the fast crack propagation

In this section, we focus on the discussion for the 'phase' of fast crack propagation. To explore the inertia effect caused by the fast crack propagation, the specimen is designed under the action of constant load $p(t) = p_0$ rather than time varying load, but the crack grows with high speed in this case. The problem for fast crack propagation is a nonlinear problem, because one part of the boundaries—the crack—has unknown length beforehand; for this moving boundary problem, we must give additional condition for determining the solution. That is, we must give a criterion checking crack propagation or crack arrest at the growing crack tip. There are different methods, e.g. the critical stress criterion or critical energy criterion. The stress criterion is used in this paper: $\sigma_{yy} < \sigma_{\mathrm{c}}$ represents crack arrest, $\sigma_{yy} = \sigma_{\mathrm{c}}$ represents the critical state and $\sigma_{yy} > \sigma_{\mathrm{c}}$ represents crack propagation. The simulation of a fracturing process runs as follows.

Given the specimen geometry and its material constants we first solve the initial dynamic problem in the way previously described. When the stress σ_{yy} reaches a prescribed critical value σ_{c} the crack is extended by one grid interval. The crack now continues to grow, by one grid interval at a time, as long as the σ_{yy} stress level ahead of the propagating crack tip reaches the value of σ_{c}. During the propagation stage the time that elapses between two sequential extensions is recorded and the corresponding velocity is evaluated.

Keeping the same material constants as mentioned in section 2, the sample size in this section is $H = 20, L = 50, a_0 = 1.2$ (mm).

Firstly, we explored the average crack propagating velocity of quasicrystals and periodic crystals shown in figure 6. Assume the critical stress of quasicrystals $\sigma_{\mathrm{c}}^{q} \approx 450$ MPa (for the decagonal Al–Ni–Co quasicrystal approximately, obtained by comparing the hardness of decagonal Al–Cu–Co and Al–Ni–Co quasicrystals) and that of crystals $\sigma_{\mathrm{c}}^{\mathrm{c}} \approx 550$ MPa approximately (the critical stress of quasicrystals is smaller than that of crystals because the brittleness of quasicrystals is greater than that of crystals; for some details refer to [25] and [26]). We notice that the average velocity in quasicrystals is greater than that in the periodic crystals, which reveals that the quasicrystals are more brittle than the crystals.

Next let us look at the average velocity under different loads in quasicrystals. The above described procedure was conducted, keeping the same geometry and material constants. With various loads, the relation between average velocity and crack growth is constructed in figure 7. The average crack velocity smoothly increases with increasing loads. We think this is understandable: because the time to reach the stress criterion is shorter as the load increases, the velocity is greater.

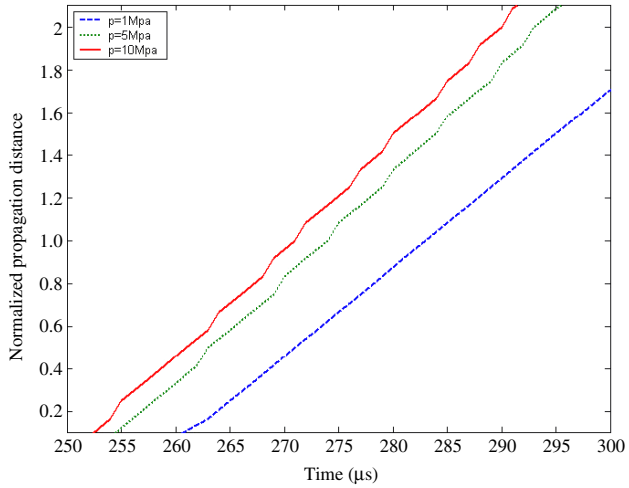

Figure 8. Normalized crack growth size $(a - a_0)/a_0$ of crack tip versus time for different load levels.

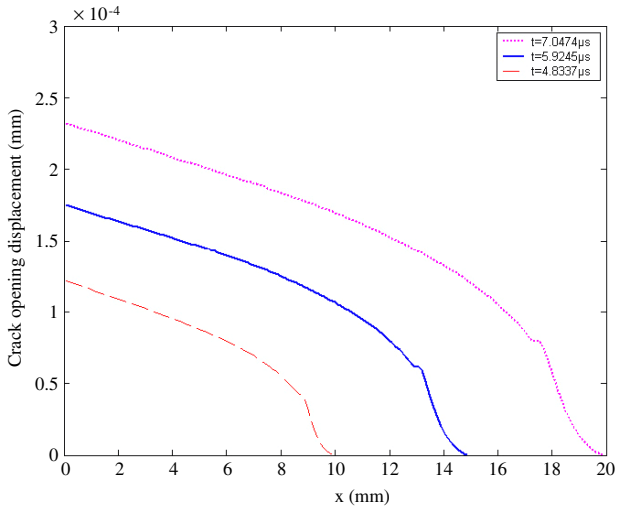

Figure 9. Geometry of the crack opening at three different time steps with $p_0 = 1$ Mpa.

Also, the picture of the growing crack, shown in figure 8, presents many steps when the load level grows. From the slope of the step, that is the speed of the crack spreading, the velocity in the process of the propagating is changing. Nonetheless, the alteration is not completely evident, as the curves in the figure 8 approximate to a straight line. The velocity remains invariable on the whole.

However, there is no observation experimentally for fast crack propagation, though Ebert *et al* [27] have made some observations by scanning tunneling microscopy for quasi-static crack growth. Because the fast propagation and quasi-static crack growth belong to two different topics, the comparison cannot be made.

Finally, the crack opening displacement, describing what the crack surface of the sample looks like, is shown in figure 9. The three curves in the figure are all like elliptic arcs.

7. Conclusion and discussion

A new version of the dynamic response of quasicrystals based on the argument of Bak as well as the argument of Lubensky *et al* is suggested; it can be seen as an elasto-/hydrodynamics model for the material, which can also be seen as a collaborating model of wave propagation and diffusion. This model is more complex than that of the pure wave propagation model in [4–10]; the analytic solution is not available, so we develop the finite difference procedure. Numerical results check the validity of wave propagation behavior of the phonon field, and diffusive behavior of the phason field, the interactions between phonons and phasons are also recorded but are quite complicated.

The formulas are applied to the analysis of dynamic initiation of crack growth and fast crack propagation for two-dimensional decagonal Al–Ni–Co quasicrystals: the displacement and stress fields around the tip of stationary and propagating cracks are revealed; the stress presents a singularity of order $r^{-1/2}$, in which r denotes the distance measured from the crack tip. For the fast crack propagation, which is a nonlinear problem—moving boundary problem, one must provide an additional condition for determining the solution. For this purpose we give a criterion for checking crack propagation/crack arrest based on the critical stress criterion. Application of this additional condition for determining the solution has helped us achieve the numerical simulation of the moving boundary value problem and reveal the crack length–time evolution.

The elasto-/hydrodynamics of icosahedral Al–Pd–Mn quasicrystals is a more interesting topic than that of decagonal Al–Ni–Co quasicrystals, but the equations and boundary conditions are more complicated; the numerical results will be reported subsequently.

The present work is carried out at macroscopic scale, i.e. in micrometers and microseconds in space and time. The dynamic instability of a propagating crack revealed by Fineberg *et al* [28, 29], Langer [30] and Ching *et al* [31] is a very important topic for the crack problem for a conventional material, and is also a very important topic for the crack problem of a quasicrystalline material; we are doing the work by combining the finite difference method and molecular dynamics simulation: the results will be reported in subsequent work.

Finally, we must point out that the order of magnitude of the results of the phason field seems much smaller than that of the phonon field; this is by no means always so: one of the reasons for this lies in the choice of boundary conditions in the present formalism, where the boundary conditions corresponding to phason field are taken to be zero (due to lack of measured data for generalized tractions, the simplest treatment is assuming the stress boundary of phason to be zero). Otherwise, if we put nonzero boundary conditions for the phason field, the computation shows that the order of magnitude of the phason variables will be greater.

Acknowledgments

This work is supported by the National Natural Science Foundation of China under grants no 10672022 and no

10372016. We thank Miss Jing Jia for her help in the implementation of computer program, and Professor H-R Trebin in the Institute of Theoretical and Applied Physics in Stuttgart University of Germany for helpful idea exchange.

References

[1] Bak P 1985 *Phys. Rev. Lett.* **4** 1517
[2] Bak P 1985 *Phys. Rev.* B **32** 5764
[3] Lubensky T C, Ramaswamy S and Toner J 1985 *Phys. Rev.* B **32** 7444
[4] Ding D H, Yang W G, Hu C Z and Wang R 1993 *Phys. Rev.* B **48** 7003
[5] Fan T Y 1999 *J. Phys.: Condens. Matter* **11** L513
[6] Zhu A Y, Fan T Y and Guo L H 2007 *J. Phys.: Condens. Matter* **19** 236216
[7] Fan T Y and Mai Y W 2003 *Eur. Phys. J.* B **31** 25
[8] Li C L and Liu Y Y 2001 *Phys. Rev.* B **63** 064203
[9] Rochal S B and Lorman L V 2000 *Phys. Rev.* B **62** 874
[10] Rochal S B and Lorman L V 2002 *Phys. Rev.* B **66** 144204
[11] Fan T Y, Wang X F, Li Wu and Zhu A Y 2008 Elasto/-hydro-dynamics of quasicrystals *Phil. Mag. Lett.* at press
[12] Cheminkov M A, Ott H R, Bianchi A, Migliori A and Darling T W 1998 *Phys. Rev. Lett.* **80** 321
[13] Jeong H C and Steinhardt P J 1993 *Phys. Rev.* B **48** 9394
[14] Walz C 2003 *Zur Hydrodynamik in Quasikristallen, Diplomarbeit Master Thesis* Universitaet Stuttgart
[15] Shmuely M and Alterman Z S 1973 *J. Appl. Mech.* **40** 902
[16] Acton Forman S 1990 *Numerical Method That (Usually) Work* (USA: The Mathematical Associate of American)
[17] Alterman Z S and Rotenberg A 1969 *Bull. Seism. Soc. Am.* **59** 347
[18] Alterman Z S and Loewenthal D 1970 *Geophys. J. R. Astron. Soc.* **20** 101
[19] Shmuely M and Peretz D 1976 *Int. J. Solids Struct.* **12** 67
[20] Shmuely M and Alterman Z S 1971 *Isr. J. Technol.* **9** 523
[21] Maue A W 1954 *Z. Angew. Math. Mech.* **14** 1
[22] Mutri V and Valliappen S 1986 *Eng. Fract. Mech.* **23** 585
[23] Chen Y M 1975 *Eng. Fract. Mech.* **7** 653
[24] Li X F, Fan T Y and Sun Y F 1999 *Phil. Mag.* A **79** 1943
[25] Mong X M, Tong B Y and Wu Y K 1994 *Acta Metall. Sin.* **30** 61 (in Chinese)
[26] Takeuchi S, Iwanaga H and Shibuya T 1991 *Japan. J. Appl. Phys.* **30** 561
[27] Ebert Ph, Feuerbacher M, Tamura N, Wollgarten M and Urban K 1996 *Phys. Rev. Lett.* **77** 3827
[28] Fineberg J, Gross S P, Marder M and Swinney H L 1991 *Phys. Rev. Lett.* **67** 457
[29] Fineberg J, Gross S P, Marder M and Swinney H L 1992 *Phys. Rev.* B **45** 5146
[30] Langer J S 1993 *Phys. Rev. Lett.* **70** 3592
[31] Ching E S C *et al* 1996 *Phys. Rev. Lett.* **76** 1087